DOI:10.26565/2312-4334-2022-1-02 ISSN 2312-4334

SIMULATION OF HEAT TRANSFER IN SINGLE-CRYSTAL LITHIUM NIOBATE IN INTERACTION WITH CONTINUOUS-WAVE LASER RADIATION[†]

Denys O. Protektor*, **Denys O. Lisin**[†]
V.N. Karazin Kharkiv National University
4, Svoboda Sq., Kharkiv, 61022, Ukraine
**Corresponding Author: d.protector@karazin.ua; [†]E-mail: d.lisin@karazin.ua*
Received December 18, 2021; revised December 18, 2021; accepted December 18, 2021

The paper presents the simulation results of heat transfer in single-crystal lithium niobate ($LiNbO_3$) in the form of cylinder of diameter $D_{LN} = 40$ mm and height $H = 60$ mm in interaction with continuous-wave laser radiation with the output power of $P = 50$ W and the wavelength of $\lambda = 1064$ nm. The density of the $LiNbO_3$ crystal is $\rho = 4659$ kg/m³; the thermal conductivity along the [001] direction is $k_{\parallel} = 4.61$ W/(m×K); the thermal conductivity in the (001) plane is $k_{\perp} = 4.19$ W/(m×K); the specific heat at constant pressure is $c_p = 601$ J/(kg×K); the absorption coefficient is $\alpha \sim 0.1$ %/cm @ 1064 nm. The laser beam propagates along the optical axis of the crystal. The laser beam intensity profile is represented as a Gaussian function, and the absorption of laser radiation of the single-crystal lithium niobate is described by Beer-Lambert's law. The numerical solution of the non-stationary heat conduction problem is obtained by meshless scheme using anisotropic radial basis functions. The time interval of the non-stationary boundary-value problem is 2 h 30 min. The results of numerical calculations of the temperature distribution inside and on the surface of the single-crystal lithium niobate at times $t = 10, 100, 1000, 7000$ s are presented. The time required to achieve the steady-state heating mode of the $LiNbO_3$ crystal, as well as its temperature range over the entire time interval, have been determined. The accuracy of the approximate solution of the boundary-value problem at the *n*-th iteration is estimated by the value of the norm of relative residual $\|\mathbf{r}\|_{\infty}$. The results of the numerical solution of the non-stationary heat conduction problem obtained by meshless method show its high efficiency even at a small number of interpolation nodes.
Keywords: heat transfer, lithium niobate, anisotropic thermal conductivity, laser radiation, non-stationary heat conduction problem, meshless method.
PACS: 44.10.+i, 77.84.Ek, 02.60.-x

INTRODUCTION

Lithium niobate ($LiNbO_3$) is a rhombohedral ferroelectric crystal. Lithium niobate is a phase of variable composition, which allows growing single-crystals with different [Li]/[Nb] ratios. Nominally pure $LiNbO_3$ crystals are usually grown from a congruent melt ([Li]/[Nb] = 48.6/51.4) by Czochralski method [1,2].

As any ferroelectric, $LiNbO_3$ crystal displays nonlinear optical effects, the piezoelectric effect, the photoelastic effect as well as the Pockels effect. The exclusive feature of lithium niobate is that it has excellent physical properties such as high electro-optic, piezoelectric and nonlinear optical coefficients, which makes it a popular material for various applications.

Due to its high electro-optic coefficients, $LiNbO_3$ crystal is used to create Pockels cells [3], electro-optic amplitude/phase modulators [4,5] and Q-switched lasers [6]. The nonlinear optical properties of lithium niobate make it possible to use it to create optical parametric oscillators [7,8] and parametric amplifiers for wide wavelength range [9,10], as well as for second harmonic generation of laser radiation with wavelength of > 1 μm [11-13].

It is known that the interaction of laser radiation with crystals in a wide range of luminous-flux densities is well described by the thermal model, according to which the whole process can be conditionally divided into several stages: 1) light absorption and energy transfer to thermal vibrations of the crystal lattice of a solid; 2) heating the crystal without destruction; 3) destruction of the crystal; 4) cooling of the crystal after the end of the interaction.

$LiNbO_3$ crystals are widely used in lasers, therefore, issues related to the study of the resistance of these crystals to laser radiation are of considerable interest.

Purpose of this work is simulation of heat transfer in single-crystal lithium niobate in interaction with continuous-wave (CW) laser radiation by meshless method.

Unlike grid methods, such as the finite element method (FEM) and the finite difference method (FDM), meshless schemes are devoid of complex and laborious process of constructing an interpolation grid within the considered domain of the boundary-value problem, which makes them computationally efficient and relatively easy to implement.

PROBLEM FORMULATION

Consider $LiNbO_3$ crystal in the form of cylinder of diameter $D_{LN} = 40$ mm and height $H = 60$ mm with the following physical properties: density is $\rho = 4659$ kg/m³; the thermal conductivity along the [001] direction is

[†] ***Cite as***: D.O. Protector, and D.O. Lisin, East. Eur. J. Phys. **1**, 10-15 (2022), https://doi.org/10.26565/2312-4334-2022-1-02

$k_{\parallel} = 4.61\ \mathrm{W}/(\mathrm{m}\times K)$; the thermal conductivity in the (001) plane is $k_{\perp} = 4.19$ W/(m×K); the specific heat at constant pressure is $c_p = 601$ J/(kg×K). The optic axis of the $LiNbO_3$ crystal is directed along the z-axis.

A laser beam with radiation power $P = 50$ W and radius $r_0 = 5$ mm passes through the crystal as shown in Fig. 1. The wavelength of laser radiation is $\lambda = 1064$ nm and the absorption coefficient of $LiNbO_3$ is $\alpha \sim 0.1$ %/cm @ 1064 nm.

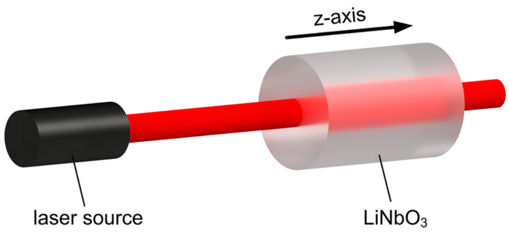

Figure 1. Passage of a laser beam through $LiNbO_3$ crystal.

When CW laser radiation interacts with a $LiNbO_3$ crystal, light is absorbed and the absorbed energy transforms into thermal energy.

The non-stationary heat conduction equation for an anisotropic solid in a closed domain can be written as follows:

$$\rho c_p \frac{\partial u}{\partial t} = \mathrm{div}\left(K\,\mathrm{grad}\,u\right) + g \tag{1}$$

where u – temperature, K – symmetric positive definite tensor of the second rank, which determines the thermal conductivity of the crystal, g – internal heat source.

At the initial moment of time, the $LiNbO_3$ crystal is at a temperature $u_0 = 25$ °C. Heat exchange with the environment occurs on the surface of the crystal. The boundary conditions for this case can be written as follows:

$$q = -h\left(u_e - u\right) \tag{2}$$

where $q = \dfrac{\partial u}{\partial \nu}$ – heat flux in anisotropic medium, $h \sim 10$ W/(m²×K) – heat transfer coefficient, $u_e = 25$ °C – ambient temperature.

The intensity of the internal heat source at depth z is described by Beer-Lambert's law:

$$g\left(x,y,z\right) = \frac{2P\alpha}{\pi r_0^2}\exp\left(-2\left(\frac{x^2+y^2}{r_0^2}\right)\right)\exp\left(-\alpha z\right) \tag{3}$$

where x, y, z – cartesian coordinates, P – radiation power, r_0 – radius of the laser beam, α – absorption coefficient.

Fig. 2 shows a visualization of the intensity of internal heat source at a depth of $z = 0.03$ m.

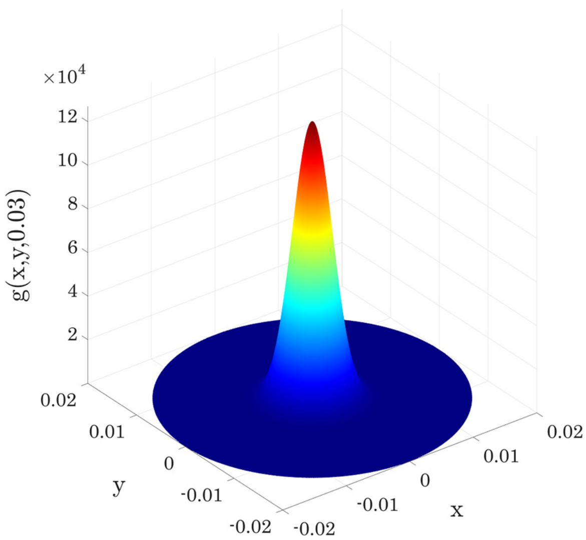

Figure 2. Visualization of the intensity of internal heat source at a depth of $z = 0.03$ m.

NUMERICAL RESULTS

The numerical solution of the considered non-stationary heat conduction problem is obtained by meshless method described in [14]. In this scheme, the dual reciprocity method (DRM) [15] with anisotropic radial basis functions (RBFs) [16] and the method of fundamental solutions (MFS) [17] are used to solve the heat conduction problem. The DRM with anisotropic RBFs is used to obtain particular solution, and the MFS is used to obtain a homogeneous solution of boundary-value problem. The time discretization of equation (1) in this method is obtained by θ-scheme [18].

The number of interpolation nodes inside and on the boundary of domain of the heat conduction problem for all calculations is $N_d = 7393$ and $N_b = 7808$, respectively. The time interval of the non-stationary boundary-value problem is 2 h 30 min.

Fig. 3 and Fig. 4 show the simulation results of the temperature field on the surface the $LiNbO_3$ crystal in interaction with CW laser radiation at different times.

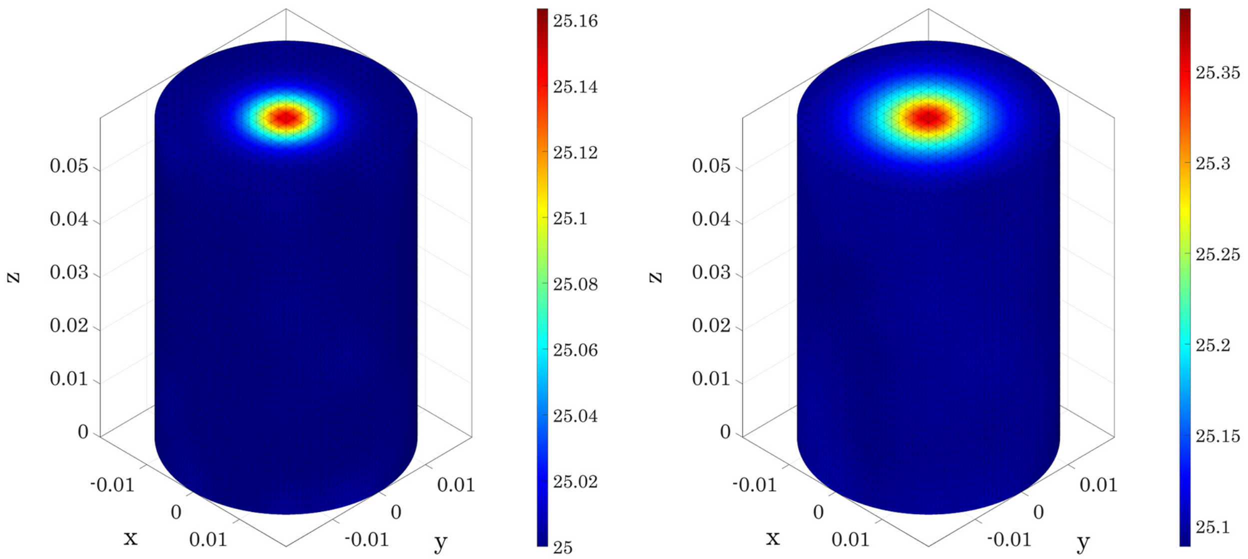

(*a*) (*b*)

Figure 3. Visualization of the temperature field on the surface the $LiNbO_3$ crystal at times $t = 10\ s$ (*a*), $t = 100\ s$ (*b*).

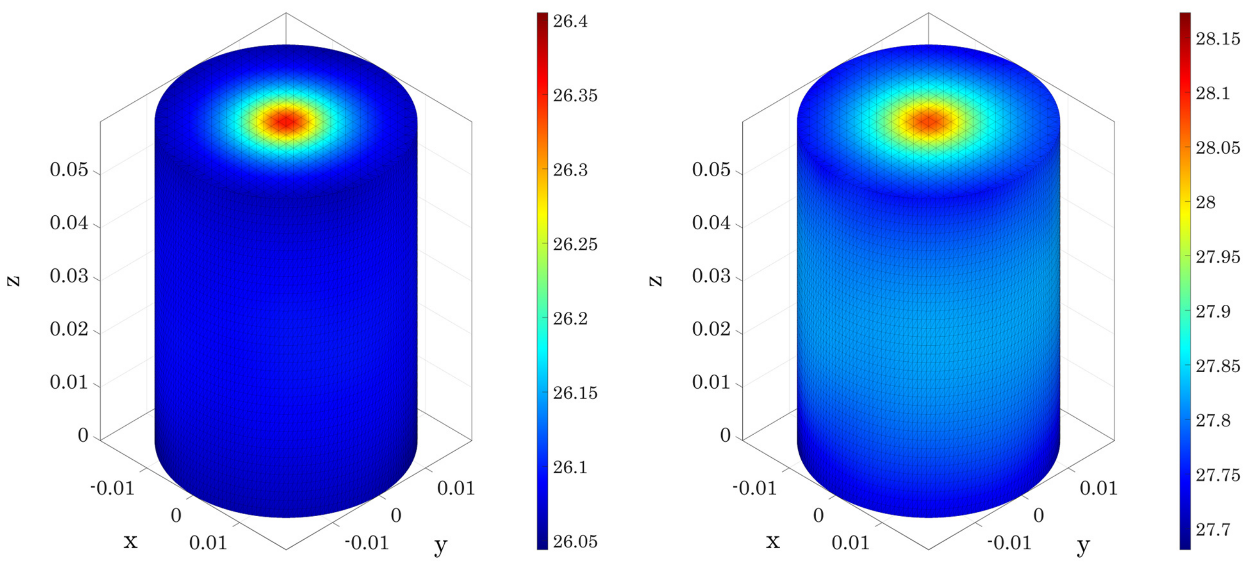

(*a*) (*b*)

Figure 4. Visualization of the temperature field on the surface the $LiNbO_3$ crystal at times $t = 1000\ s$ (*a*), $t = 7000\ s$ (*b*).

Fig. 5 and Fig. 6 show the simulation results of the temperature field inside the $LiNbO_3$ crystal in interaction with CW laser radiation at different times.

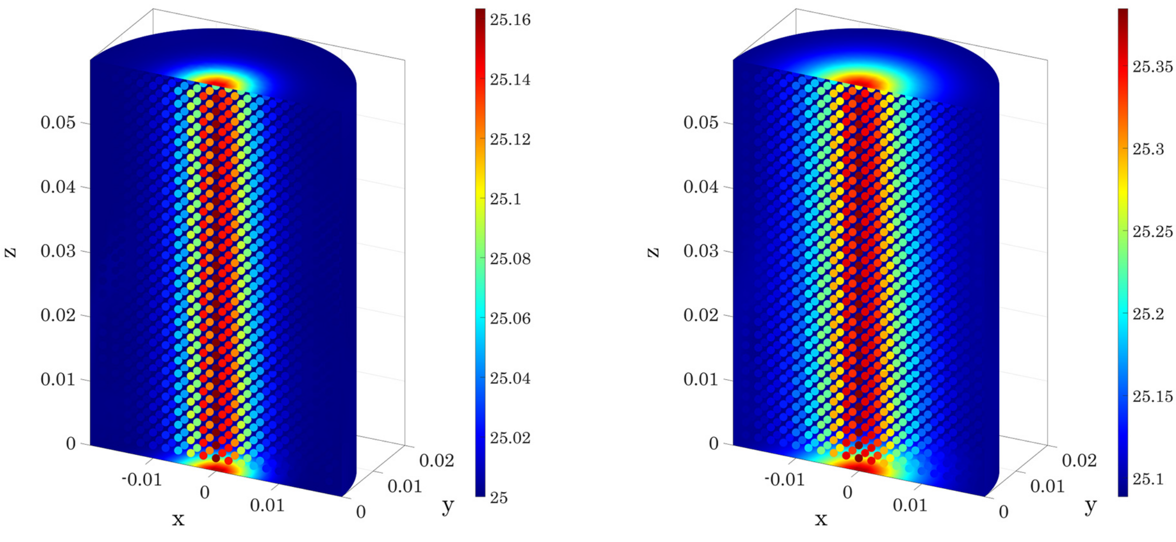

(*a*) (*b*)

Figure 5. Visualization of the temperature field inside the $LiNbO_3$ crystal at times $t = 10\ s$ (*a*), $t = 100\ s$ (*b*).

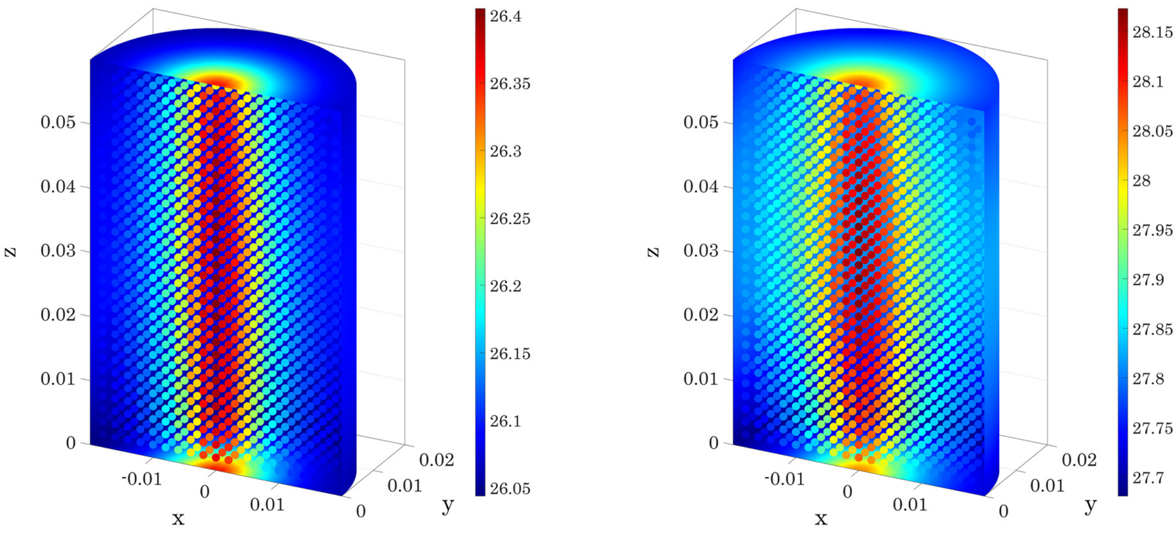

(*a*) (*b*)

Figure 6. Visualization of the temperature field inside the $LiNbO_3$ crystal at times $t = 1000\ s$ (*a*), $t = 7000\ s$ (*b*).

As one can see in Fig. 5 and Fig. 6, with time of irradiation of the crystal, the heated zone inside of the crystal expands and its temperature increases. This process continues until a steady-state thermal regime is reached. Fig. 7 shows the plot of the heating process of the $LiNbO_3$ crystal in time.

As it was shown Fig. 7, at first the temperature of the crystal increases very fast, and then the rate of increase slows down, and after about 2 h 30 min it goes into a steady-state. The time 35 min, when the crystal temperature reaches 63.2% of the steady-state value is the thermal time constant τ.

The thermal time constant is calculated as follows:

$$\tau = \frac{\rho V c_p}{h A_s} \tag{4}$$

where ρ – crystal density, V – crystal volume, c_p – specific heat at constant pressure, h – heat transfer coefficient, A_s – crystal surface area.

To estimate the accuracy of the approximate solution at the *n*-th step, we calculate the norm of relative residual:

$$\|\mathbf{r}\|_\infty = \max_{i=1,\dots,N} |r_i| \tag{5}$$

where $N = N_d + N_b$ – total number of interpolation nodes, r_i – relative residual of the approximate solution at the *i*-th node.

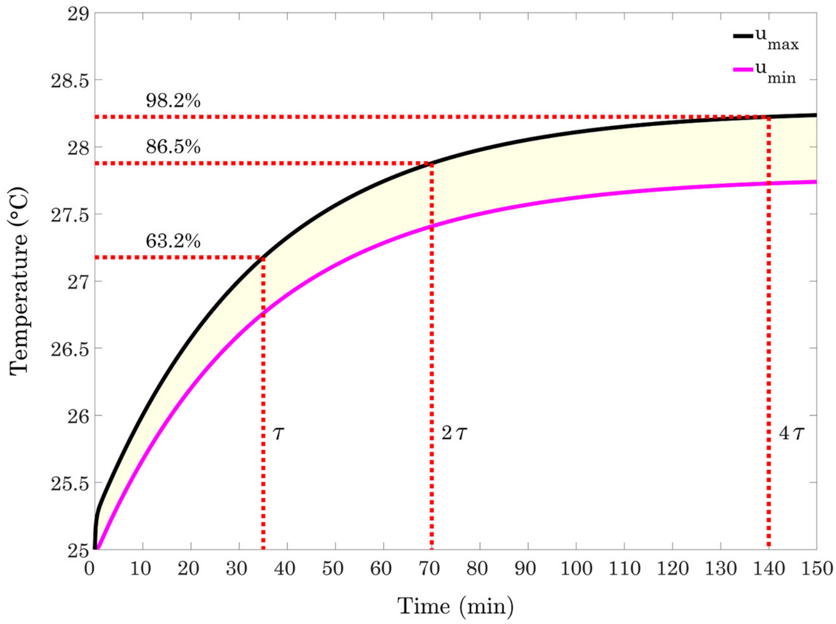

Figure 7. Plot of the heating process of the $LiNbO_3$ crystal, where u_{max} – maximum temperature of the crystal, u_{min} – minimum temperature of the crystal, τ – thermal time constant.

Fig. 8 shows plot of the change of the norm of relative residual of the approximate solution of the considered boundary-value problem.

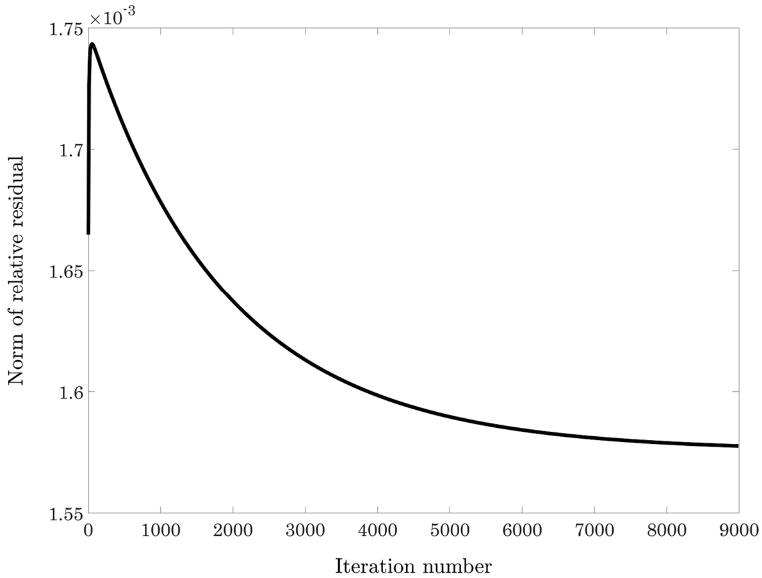

Figure 8. Plot of change of the norm of relative residual

The total estimated simulation time for a non-stationary heat conduction problem is 2303 s, which is comparable to the simulation time when using other numerical methods for solving boundary-value problems.

CONCLUSIONS

This paper presents the simulation results of heat transfer in single-crystal lithium niobate in interaction with CW laser radiation with the output power of 50 W and the wavelength of 1064 nm. The time interval of the non-stationary boundary-value problem was 2 h 30 min. It is defined, that after about 4τ the temperature of the crystal goes into a steady-state, and is in the range of 27.74 to 28.24 °C. The results of numerical calculations of the temperature distribution inside and on the surface of the single-crystal lithium niobate at times $t = 10$, 100, 1000, 7000 s are presented.

The numerical solution of the non-stationary heat conduction problem is obtained by meshless scheme using anisotropic radial basis functions. The accuracy of the approximate solution of the boundary-value problem at a specified time interval is estimated by the value of the norm of relative residual, and in the worst case is 1.74348×10^{-3}. The lower values of the norm of relative residual are in the range from 2.05119×10^{-14} to 1.25433×10^{-9}. The numerical simulation results obtained using the meshless method are in good agreement with the results obtained using the FEM, which indicates the high efficiency of the meshless scheme even at a small number of interpolation nodes.

ORCID IDs

Denys O. Protektor, https://orcid.org/0000-0003-3323-7058; **Denys O. Lisin,** https://orcid.org/0000-0002-6718-7389

REFERENCES

[1] H.H. Kusuma, D.P.N. Made, M.R. Sudin, and M.S. Rohani, AIP Conference Proceedings. **1217**(1), 182-186 (2010), https://doi.org/10.1063/1.3377808.
[2] M. Kosmyna, B. Nazarenko, V. Puzikov, and A. Shekhovtsov, Acta Physica Polonica A. **124**, 305-313 (2013), http://dx.doi.org/10.12693/APhysPolA.124.305.
[3] K.A. Nelson, N. Edwards, M.J. Harrison, A. Kargar, W.J. McNeil, R.A. Rojeski, and D.S. McGregor, Nuclear Instruments and Methods in Physics Research Section A: Accelerators, Spectrometers, Detectors and Associated Equipment. **620**, 363-367 (2010), https://doi.org/10.1016/j.nima.2009.12.042.
[4] M. Zhang, C. Wang, P. Kharel, D. Zhu, and M. Lončar, Optica. **8**(5), 652-667 (2021), https://doi.org/10.1364/OPTICA.415762.
[5] T. Sakamoto, T. Kawanishi, and M. Izutsu, Opt. Lett. **31**(6), 811-813 (2006), https://doi.org/10.1364/OL.31.000811.
[6] H. Jelínková, J. Šulc, P. Koranda, M. Němec, M. Čech, M. Jelínek, and V. Škoda, Laser Physics Letters. **1**(2), 59-64 (2004), http://dx.doi.org/10.1002/lapl.200310020.
[7] D.W. Michael, K. Kolenbrander, and J.M. Lisy, Review of Scientific Instruments. **57**(6), 1210-1212 (1986), https://doi.org/10.1063/1.1138632.
[8] C. Yu, and A. Kung, J. Opt. Soc. Am. B. **16**(12), 2233-2238 (1999), https://doi.org/10.1364/JOSAB.16.002233.
[9] T. Kishimoto, K. Inafune, Y. Ogawa, N. Sekine, H. Murai, and H. Sasaki, in: *Integrated Optics: Devices, Materials, and Technologies XXIII*, edited by S.M. García-Blanco (SPIE, San Francisco, 2019), https://doi.org/10.1117/12.2507784.
[10] D. Andreou, Optics Communications. **27**(1), 171-176 (1978), https://doi.org/10.1016/0030-4018(78)90200-6.
[11] B.H. Ahn, W.W. Clark III, R.R. Shurtz II, and C.D. Bates, J. Appl. Phys. **54**(3), 1251-1255 (1983), https://doi.org/10.1063/1.332187.
[12] O. Sánchez-Dena, Z. Behel, E. Salmon, E. Benichou, J.-A. Reyes-Esqueda, P.-F. Brevet, and C. Jonin, Opt. Mater. **107**, 110169 (2020), https://doi.org/10.1016/j.optmat.2020.110169.
[13] R. Debnath, P. Kumari, and A. Saha, Optik. **132**, 232-235 (2017), https://doi.org/10.1016/j.ijleo.2016.12.049.
[14] D.O. Protektor, V.M. Kolodyazhny, D.O. Lisin, and O.Yu. Lisina, Cybern. Syst. Anal. **57**, 470-480 (2021), https://doi.org/10.1007/s10559-021-00372-8.
[15] M.S. Ingber, C.S. Chen, and J.A. Tanski, Int. J. Numer. Methods Eng. **60**(13), 2183-2201 (2004), https://doi.org/10.1002/nme.1043.
[16] Wen Chen, Zhuo-Jia Fu, and C.S. Chen, *Recent Advances in Radial Basis Function Collocation Methods*, 1st ed. (Springer, Berlin, 2014), pp. 21-22.
[17] A. Bogomolny, SIAM J. Numer. Anal. **22**(4), 644-669 (1985), https://www.jstor.org/stable/2157574.
[18] H.P. Langtangen, and S. Linge, *Finite Difference Computing with PDEs*, 1st ed. (Springer, Cham, 2017), pp. 226-227.

МОДЕЛЮВАННЯ ТЕПЛООБМІНУ В МОНОКРИСТАЛІЧНОМУ НІОБАТІ ЛІТІЮ ПРИ ВЗАЄМОДІЇ БЕЗПЕРЕВНИМ ЛАЗЕРНИМ ВИПРОМІНЕНИЯМ

Денис О. Протектор, Денис О. Лісін
Харківський національний університет імені В. Н. Каразіна
м. Свободи, 4, Харків, Україна

У статті представлені результати моделювання теплового процесу, який протікає в монокристалі ніобату літію ($LiNbO_3$) у формі циліндра діаметром $D_{LN} = 40$ мм та висотою $H = 60$ мм при взаємодії з безперервним лазерним випромінюванням потужністю $P = 50$ Вт та довжиною хвилі $\lambda = 1064$ нм. Щільність кристала $LiNbO_3$ $\rho = 4659$ кг/м^3; теплопровідність вздовж напрямку [001] $k_{\parallel} = 4.61$ Вт/(м×К), теплопровідність у площині (001) $k_{\perp} = 4.19$ Вт/(м×К); питома теплоємність при постійному тиску $c_p = 601$ Дж/(кг×К); коефіцієнт поглинання $\alpha \sim 0.1$ %/см @ 1064 нм. Лазерний пучок проходить вздовж оптичної осі кристала. Профіль інтенсивності лазерного пучка представляється у вигляді функції Гауса, а поглинання лазерного випромінювання кристалом ніобату літію описується законом Бугера-Ламберта. Чисельний розв'язок нестаціонарної задачі теплопровідності здійснюється за безсітковою схемою з використанням анізотропних радіальних базисних функцій. Часовий інтервал, на якому розв'язується нестаціонарна задача теплопровідності, становить 2 год 30 хв. Наведено результати числових розрахунків розподілу температурного поля всередині та на поверхні кристала ніобату літію в моменти часу $t = 10, 100, 1000, 7000$ с. Визначено час, протягом якого досягається сталий режим нагрівання кристала $LiNbO_3$, а також його температурний діапазон на всьому часовому інтервалі. Точність наближеного розв'язку крайової задачі на n-му кроці оцінюється за величиною норми відносної нев'язки $\|\mathbf{r}\|_{\infty}$. Результати чисельного розв'язку нестаціонарної задачі теплопровідності, отримані з використанням безсіткового методу, свідчать про його високу ефективність вже на невеликій кількості інтерполяційних вузлів.

Ключові слова: тепловий процес, ніобат літію, анізотропна теплопровідність, лазерне випромінювання, нестаціонарна задача теплопровідності, безсітковий метод.